

## Single particle dynamics in a radio-frequency produced plasma sheath

M. Rubin-Zuzic, V. Nosenko, S. Zhdanov, A. Ivlev, H. Thomas, S. Khrapak, and L. Couedel

Citation: [AIP Conference Proceedings](#) **1925**, 020023 (2018);

View online: <https://doi.org/10.1063/1.5020411>

View Table of Contents: <http://aip.scitation.org/toc/apc/1925/1>

Published by the [American Institute of Physics](#)

---

### Articles you may be interested in

[Laser-stimulated melting of a two-dimensional complex plasma crystal](#)

[AIP Conference Proceedings](#) **1925**, 020016 (2018); 10.1063/1.5020404

[Particle detection algorithms for complex plasmas](#)

[AIP Conference Proceedings](#) **1925**, 020010 (2018); 10.1063/1.5020398

[Supersonic particle in a low damped complex plasma under microgravity conditions](#)

[AIP Conference Proceedings](#) **1925**, 020006 (2018); 10.1063/1.5020394

[Excitation of nonlinear wave patterns in flowing complex plasmas](#)

[AIP Conference Proceedings](#) **1925**, 020015 (2018); 10.1063/1.5020403

[Ekoplasma — Experiments with grid electrodes in microgravity](#)

[AIP Conference Proceedings](#) **1925**, 020004 (2018); 10.1063/1.5020392

[Particle velocity distribution in a three-dimensional dusty plasma under microgravity conditions](#)

[AIP Conference Proceedings](#) **1925**, 020005 (2018); 10.1063/1.5020393

---

# Single Particle Dynamics in a Radio-Frequency Produced Plasma Sheath

M. Rubin-Zuzic<sup>1,a)</sup>, V. Nosenko<sup>1</sup>, S. Zhdanov<sup>1</sup>, A. Ivlev<sup>2</sup>, H. Thomas<sup>1</sup>, S. Khrapak<sup>3</sup>  
and L. Couedel<sup>3</sup>

<sup>1</sup> *Deutsches Zentrum für Luft- und Raumfahrt, Institut für Materialphysik im Weltraum,  
Gruppe Komplexe Plasmen, 82234 Weßling, Germany*

<sup>2</sup> *Max Planck Institut für extraterrestrische Physik, 85748 Garching, Germany*

<sup>3</sup> *CNRS, Aix-Marseille Univ., PIIM, UMR 7345, 13397 Marseille cedex 20, France*

<sup>a)</sup> *milenko.rubin-zuzic@dlr.de*

**Abstract.** Recently different research groups have investigated the motion of a single dust particle levitated in a rf plasma. Here we describe a highly resolved experiment where a single spherical melamine formaldehyde microparticle is suspended in the plasma sheath above the lower electrode of a capacitively coupled radio-frequency discharge at controlled pressure, power and neutral gas flow rate. The particle's horizontal oscillation is investigated, from which its neutral gas damping rate, kinetic temperature and eigenfrequency of the potential trap are measured. Compared to prior experiments we report about inhomogeneous and anisotropic velocity variations.

## INTRODUCTION

The investigation of single suspended microparticles in a plasma can be used to study the properties of the particle as well as of local plasma environment. The motion of a single particle in a rf plasma is similar to the Brownian motion [1], originating from random collisions between the particle and the surrounding neutral gas atoms. In addition disturbances and anisotropic and inhomogeneous particle vibrations have to be considered which lead to an enhanced particle temperature above the room temperature [2,3,4]. They originate from, e.g., electric field fluctuations, dust charge fluctuations, gas flow fluctuations and interaction of the dust particle with the illuminating laser beam. In the simplified case of a particle trapped in a potential well and interacting with the surrounding medium by friction in the presence of a varying driving force the Uhlenbeck–Ornstein–Wang model [5,6] can be adopted. Its solution gives an expression for the mean squared displacement from which the particle temperature can be obtained, assuming ballistic motion for small time scales. The fit of the measured resonance profile to a driven damped harmonic oscillator yields information about the resonance frequency as well the frictional damping rate [7].

## EXPERIMENT

Our experiment was conducted in a modified GEC (Gaseous Electronics Conference) rf reference cell [8,9]. The plasma was produced using a capacitively coupled rf discharge in argon at a pressure of 1.36 Pa. The power was adjusted to 1 W and the gas flow was set to 0.2 sccm. An aluminium ring of 3 cm in diameter (1 mm height and thickness) was placed on the center of the lower electrode. This modifies the electrostatic potential and produces a parabolic potential trap.

Before performing the experiments we determined the magnification of our optical system. For this purpose we used a USAF1951 test chart [10], which was placed at 1 cm height. A pixel size of  $1.881 \pm 0.004 \mu\text{m}$  was measured.

A single dust particle was suspended and confined in the plasma sheath about 1 cm above the lower rf electrode at the center of the aluminium ring. The microsphere was made of melamine formaldehyde and had a diameter of  $9.19 \pm 0.09 \mu\text{m}$  ( $\rho = 1510 \text{ kg/m}^3$ ,  $m = 6.137 \cdot 10^{-13} \text{ kg}$ ).

For the illumination of the particle we used a thin horizontal laser sheet of about 100  $\mu\text{m}$  thickness. The scattered light was recorded with a combination of a long-distance microscope (Questar QM100, [11]) and a CMOS camera (Photron, 4 Megapixels, 12 bit sensor, [12]). A frame rate of 60 Hz was used and the laser power was adjusted in order to collect enough light on the chip and avoid overexposition of the CMOS chip, which is important for a sub-pixel measurement of the particle position.

By moving the horizontal laser sheet vertically and an additional vertical laser sheet horizontally we could verify that only a single particle has been trapped.

## DATA ANALYSIS

### Particle positions and velocities

A set of 2726 images was recorded with 8 bit gray scale resolution at 60 Hz. For particle detection the global noise was subtracted and the remaining particle spot was used to measure its positions from intensity weighted center of mass positions of the contributing pixels.

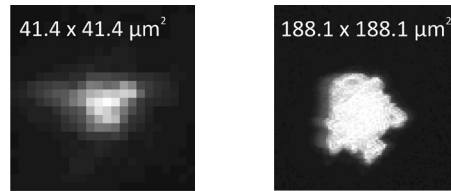


**FIGURE 1.** Left: a particle spot consisting of single gray scaled pixels. Right: the superposed particle trace over 45 s.

From our analysis of the fractional parts of the measured coordinates, no pixel locking was found — the fractional parts are nearly randomly distributed, with a mean value of  $(0.496, 0.487) \pm (0.293, 0.294)$  without duplicates. The difference in particle positions measured using 8bit and 16bit gray scale images is negligible, the Pearson's correlation coefficient is greater than 0.999 for the x and y components.

The particle velocity was calculated from particle positions measured between next neighboring images. It is randomly varying versus time with a mean value of  $1.28 \cdot 10^{-4} \pm 6.3 \cdot 10^{-5}$  m/sec. Comparison for 8 and 16bit images gives for the mean velocity a very good agreement:  $\frac{\langle v_{8bit} \rangle}{\langle v_{16bit} \rangle} = 0.998$ .

### Resonance profile

The resonance profile (oscillation amplitude vs. frequency) was obtained from the discrete Fast Fourier Transform (FFT) of the time varying 2d coordinates. In Fig. 2 the blue curve shows the FFT and the red curve represents a fit to the amplitude variation of a driven damped harmonic oscillator. From the fit we obtain a resonance frequency of  $f_0 = 1.26$  Hz and a frictional gas damping time constant of  $\tau = m/k = 0.43$  s [7]. Theoretical estimation of the Epstein frictional time [13] gives  $\tau = 0.56$  s computed with a Millikan coefficient of 1.39. To obtain the same Epstein frictional time as in the experiment the particle diameter should be reduced to 7.06  $\mu\text{m}$ .

### Temperature Measurement

Assuming that the random movement of a single microparticle can be treated as Brownian motion we can calculate the mean squared displacement (MSD) as presented in Fig. 3. For a particle which is confined in a harmonic potential well the MSD solution is given by the Uhlenbeck–Ornstein–Wang model [5,6], whereby

$\langle \Delta r^2 \rangle = \frac{4k_B T}{m\omega_0^2} \left[ 1 - \exp\left(\frac{-\beta t}{2}\right) \left( \cos \omega_1 t + \frac{\beta}{2\omega} \sin \omega_1 t \right) \right]$  with  $\omega_1 = \sqrt{\omega^2 - \frac{\beta^2}{4}}$ . For small times scales, where  $t \cdot \beta \ll 1$ , the particle moves ballistically and the MSD solution reduces to  $\langle \Delta r^2 \rangle = 2k_B T/m \cdot t^2$ . From a fit with the first two data points we obtain a mean particle temperature of  $T = 441.4$  K. Due to various disturbances (e.g., charge fluctuations, electric field fluctuations, variation of gas flow) this value is higher than the room temperature.

Differently from prior investigations, we observe an inhomogeneous oscillation for larger times with varying frequency and amplitude. Therefore, the theoretical MSD solution is not applicable for our measurement with long time span.

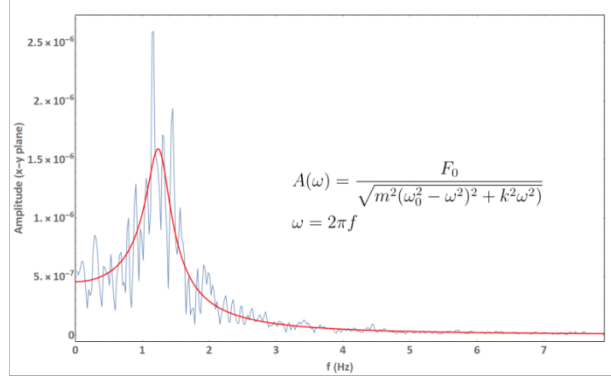


**FIGURE 2.** Oscillation amplitude  $A(\omega)$  versus frequency from FFT (blue) of particle coordinates with a fit to damped harmonic oscillator (red) [7].

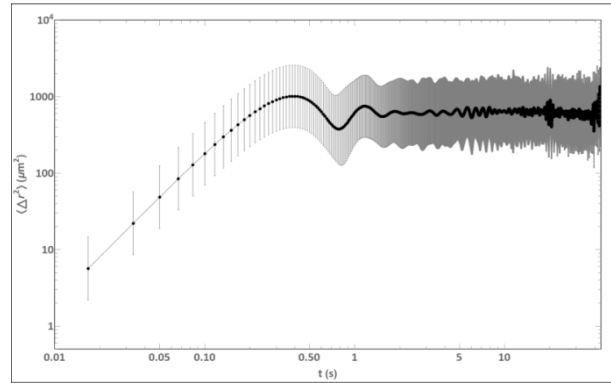


**FIGURE 3.** Mean squared displacement as function of time (mean value and standard deviation).

## Inhomogeneities and Anisotropy

To investigate deviations between measurements (see Fig. 3) and the MSD solution given by the Uhlenbeck–Ornstein–Wang model, we calculated separately for  $x$  and  $y$  coordinates the resonance frequency, damping time, probability density function, energy distribution, autocorrelation function and MSD. We find in all cases differences for the two axes:

**TABLE 1.** Parameters obtained separately for  $x$  and  $y$  coordinates.

coordinates	resonance frequency $f_0$	frictional drag time $\tau$	temperature from MSD
$x$	1.22 Hz	$\tau=0.39$ s	367.8 K
$y$	1.30 Hz	$\tau=0.37$ s	515.0 K

The particle is oscillating mainly horizontally around its equilibrium position in a parabolic-like potential trap above the lower electrode. The oscillations in  $x$  and  $y$  are inhomogeneous and not in phase. The velocity autocorrelation decreases up to 2.5 s as expected; above a long range correlation is measured, originating from unknown driving sources.

The distribution of  $x$  and  $y$  velocities is deviating from a Gaussian distribution, whereby the distribution for  $v_x$  is narrower than for  $v_y$ . For both curves the variance and standard deviation were measured. The slope of  $\text{Ln}(v_{x,y})$  is constant, showing that the distribution curves are as expected proportional to  $v_{x,y}^2$ . The different slopes show that the temperature in  $y$  direction is higher (Figure 4).

The resonance frequency in  $y$  direction is 0.08 Hz higher, indicating that the potential trap is anisotropic, possibly elliptically shaped. The temperature is significantly higher for the  $y$  direction.

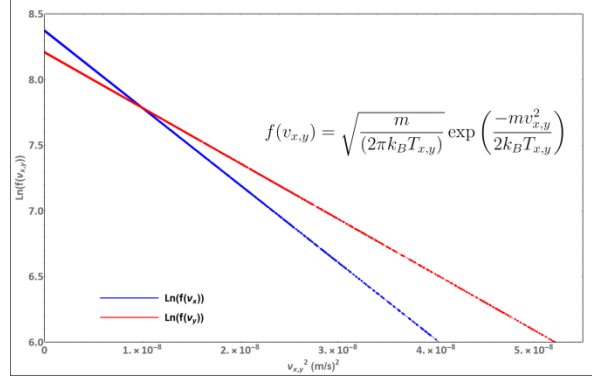


**FIGURE 4.** Energy distribution for x and y coordinates, showing for each component a nearly perfect linear variation of  $\text{Ln}(f(v_{x,y}))$  versus velocity squared as predicted by a Gaussian profile.  $f(v_{x,y})$  is the probability distribution function for the corresponding velocity component.

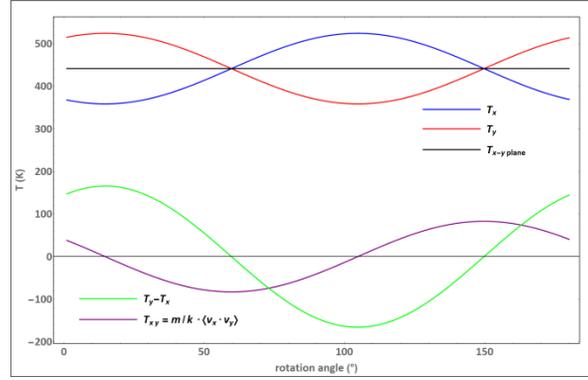


**FIGURE 5.** The curves show measured temperatures versus rotation angle determined from the MSD for the x and y coordinates and the planar movement. In addition the temperature difference  $T_y - T_x$  and the cross-correlation part of the temperature are plotted.

Neutralization of the measured anisotropic oscillation in x and y direction can be obtained by rotation of all particle coordinates by  $58.7^\circ$  or  $148.7^\circ$ . For these angles the same temperatures of  $T_x = T_y = 441.4$  K is measured.  $T_x$  and  $T_y$  are varying sinusoidally with a phase difference of  $90^\circ$  around the mean value of 441.4 K. The temperature difference oscillates between 147.2 K and  $-147.2$  K [14].

The cross-correlation part of the temperature ( $T_{xy}$ ) is not vanishing as one would expect. It has a sinusoidal shape with a phase shift of  $90^\circ$  respective to the variation of  $T_x$  and  $T_y$  (Figure 6).

To investigate the angle dependency in our experiment we performed numerical simulations for random walk processes. These simulations demonstrate that in general the cross-correlation temperature depends on the diffusion coefficient. Here we find that the larger the diffusion coefficient is the greater is the cross-correlation temperature. For small diffusion the mean cross-correlation temperature vanishes, which we would expect for our experiment.

## SUMMARY

The movement of a single randomly oscillating microsphere in a rf plasma sheath was recorded with a long-distance microscope and a high-resolution camera. We measured particle positions, velocities, FFT spectra, velocity autocorrelation and mean squared displacement. The investigations yield a particle's mean kinetic temperature of 441.4 K, frictional gas damping time of 0.43 s and potential trap eigenfrequency of 1.26 Hz.

Different aspects will be investigated in future to study the origin of the inhomogeneous and anisotropic oscillation of the particle leading to angle dependent temperatures along the x and y direction and an associated considerable contribution of the cross-correlation temperature: a) variations of the DC potential of the lower electrode, b) presence and variation of directed gas flow, c) asymmetric horizontal potential trap.

## ACKNOWLEDGMENT

This work was supported by the French–German PHC PROCOPE Program (Project No. 35325NA/57211784). S.A.K. was supported by the A\*MIDEX project (Nr. ANR-11-IDEX-0001-02) funded by the French Government “Investissements d’Avenir” program managed by the French National Research Agency (ANR).

## REFERENCES

1. A. Einstein, *Ann. Phys. (Berlin)* 322, 549–560 (1905)
2. C. Schmidt and A. Piel, *Phys. Rev. E* 92, 043106 (2015)
3. C. Schmidt and A. Piel, *Phys Plasmas* 23, 083704 (2016); doi: 10.1063/1.4960320
4. J. Kong, K. Qiao, L.S. Matthews and T.W. Hyde, *J. Plasma Phys.* 82 (2016), 905820505, doi:10.1017/S0022377816000842
5. G. E. Uhlenbeck and L. S. Ornstein, *Phys. Rev.* 36, 823 (1930)
6. M. C. Wang and G. E. Uhlenbeck, *Rev. Mod. Phys.* 17, 323 (1945)
7. M. Zuzic, *J. Vac. Sci. Technol. A* 14(2) (1996)
8. V. Nosenko, A.V. Ivlev and G. E. Morfill, *PRL* 108, 135005 (2012)
9. L. Couedel, V. Nosenko, A.V. Ivlev, S. K. Zhdanov, H. M. Thomas and G. E. Morfill, *PRL* 104, 195001 (2010)
10. MIL-STD-150A, 5.1.1.7, Resolving Power Target (1951), <http://www.dtic.mil/dtic/tr/fulltext/u2/a345623.pdf>
11. Company Seven, [http://www.company7.com/library/questar/QM\\_100\\_30003c7.pdf](http://www.company7.com/library/questar/QM_100_30003c7.pdf)
12. Photron, <https://photron.com/high-speed/cameras/fastcam-mini-wx100/>
13. P.S. Epstein, *Phys. Rev.* 23, 710–733 (1924)
14. V. Dotsenko, A. Maciołek, O. Vasilyev and G. Oshanin, *Phys. Rev. E* 87, 062130 (2013)